AD NUMBER

AD131947

NEW LIMITATION CHANGE

TO

Approved for public release, distribution unlimited

FROM

Distribution authorized to U.S. Gov't. agencies and their contractors; Administrative/Operational Use; 19 Mar 1957. Other requests shall be referred to Naval Ordnance Lab., White Oak, MD.

AUTHORITY

NOL ltr, 29 Aug 1974

NAVORD REPORT 4438

A PROCEDURE FOR CALCULATING THE BOUNDARY-LAYER DEVELOPMENT IN THE REGION OF TRANSITION FROM LAMINAR TO TURBULENT FLOW

19 MARCH 1957

U. S. NAVAL ORDNANCE LABORATORY
WHITE OAK, MARYLAND

NAVORD Report 4438

Aeroballistic Research Report 367

A PROCEDURE FOR CALCULATING THE BOUNDARY-LAYER DEVELOPMENT IN THE REGION OF TRANSITION FROM LAMINAR TO TURBULENT FLOW

Prepared by:

Jerome Persh

ABSTRACT: A method for calculating the development of the boundary layer in the region of transition from laminar to turbulent flow is given. This method is based on empirical correlations of a large amount of experimental velocity profile data in the transition region for incompressible and compressible flows with and without pressure gradients. The velocity profile correlations and an assumed skin-friction law are used in conjunction with the boundary-layer momentum equation to predict the development of the boundary-layer parameters. Within the framework of the assumptions the method is valid for incompressible and compressible flows with and without pressure gradients and heat transfer. Several examples are given which illustrate the boundary-layer profile history in the transition region of general body shapes.

U. S. NAVAL ORDNANCE LABORATORY
WHITE OAK, MARYLAND

This report contains the results of an analytical investigation of the boundary layer in the region of transition from laminar to turbulent flow. This work was undertaken to develop a calculation scheme to bridge the gap between laminar and turbulent flow. Since the procedure outlined herein is principally intended for arbitrary body shapes, its usefulness will be most apparent for missile applications. The results obtained are of practical importance in the design of current and forthcoming high-speed missiles.

This work was carried out under Task Number 502-825/51014/01. The author is indebted to Dr. R. K. Lobb for his continued interest during the course of the investigation, Mr. I. Korobkin for significant suggestions and comments, and to Mr. Richard Buck who carried out the extensive calculations associated with the NOL Pressurized Range Data.

WILLIAM W. WILBOURNE
Captain, USN
Commander

H. H. KURZWEG
By direction

CONTENTS

ILLUSTRATIONS

SYMBOLS

c_f = local skin-friction coefficient based on free-stream properties, $2\tau_w/\rho_e u_e^2$

c_{fw} = local skin-friction coefficient based on wall properties, $2\tau_w/\rho_w u_e^2$

c_p = specific heat at constant pressure

h = local heat-transfer coefficient

H = boundary-layer shape parameter, δ^*/θ

H_{inc} = boundary-layer shape parameter for incompressible flow $\delta^*_{inc}/\theta_{inc}$

k = thermal conductivity

Nu = Nusselt number, hx/k

$\bar{n}$ = exponent in power law velocity profile representation

p = pressure

p_o' = stagnation pressure

Pr = Prandtl number

q = rate of heat transfer per unit area

R = radius of axisymmetric body

Re_θ = Reynolds number based on momentum thickness, $\rho_e u_e \theta/\mu_e$

Re_w = Reynolds number based on distance and wall properties, $\rho_w u_e s/\mu_w$

s = distance along surface from stagnation point

T = temperature

T_o' = stagnation temperature

u = mean velocity component in s-direction

δ = total boundary-layer thickness

δ^*_{inc} = displacement thickness for incompressible flow

$$\delta^*_{inc} = \int_0^{\delta} (1 - \frac{u}{u_e})\, dy$$

δ^* = displacement thickness for compressible flow

$$\delta^* = \int_0^{\delta} (1 - \frac{\rho u}{\rho_e u_e})\, dy$$

θ_{inc} = momentum thickness for incompressible flow

$$\theta_{inc} = \int_0^{\delta} \frac{u}{u_e} (1 - \frac{u}{u_e})\, dy$$

θ = momentum thickness for compressible flow

$$\theta = \int_0^{\delta} \frac{\rho u}{\rho_e u_e} (1 - \frac{u}{u_e})\, dy$$

α = angle between normal to surface of a given body and flow direction

γ = ratio of specific heats

ρ = density

μ = viscosity

ω = exponent in viscosity temperature relationship

Subscripts:

ad = equilibrium wall temperature for zero heat transfer

e = values based on local free-stream conditions outside boundary layer

inc = incompressible flow

Lam = laminar flow

max = maximum value

TR = transition region

Turb = turbulent flow

w = values based on wall conditions

∞ = values based on conditions ahead of normal shock wave

A PROCEDURE FOR CALCULATING THE BOUNDARY-LAYER DEVELOPMENT IN THE REGION OF TRANSITION FROM LAMINAR TO TURBULENT FLOW

INTRODUCTION

1. Probably the weakest link in the calculations of wall temperatures and heat transfer to arbitrary body shapes is the location of the transition "point". Numerous theoretical investigations (for example references a, b, and c) of laminar boundary-layer stability and experimental investigations (references d, e, and f as examples) have been conducted in an effort to predict the location of transition for arbitrary bodies and free-stream conditions. Despite these extensive investigations, a quantitative means for determining the transition location is still not available. Although it is shown in the thorough investigation of experimental transition data conducted by Probstein and Lin (reference g) that the qualitative trends predicted by stability calculations are more or less verified by experiments, little can be concluded as far as quantitative information is concerned.

2. Another serious deficiency in the current calculation schemes is the neglect of the transition region. The usual procedure is to terminate the laminar boundary-layer calculations at an assumed transition point and from this point on downstream, it is assumed that fully turbulent flow exists. While this procedure yields a conservative result from a heat transfer standpoint, it is conceivable that configurations that are actually acceptable may be rejected because of excessive conservatism due to this technique. Since the behavior of the boundary layer on a given body shape depends on a complicated combination of such parameters as the geometry, pressure gradient, heat transfer, etc., cases may arise where the surface is almost entirely covered by transition region flow. On the other hand, it is reasonable to suppose that body shapes may be devised that encourage the existence of transition region flow. Consequently, since the heat transfer due to a transitional boundary layer can be substantially less than that for a fully turbulent boundary layer, this procedure may provide a means for alleviating serious heat transfer situations.

3. The present investigation was therefore inaugurated to determine whether or not a method for calculating the boundary-layer development in the transition region could be devised with the experimental and analytical information at hand. It was found that, when the boundary-layer momentum equation is used in conjunction with empirical correlations of a large

amount of velocity profile data (reference h), reasonable predictions of the boundary-layer behavior in the transition region could be made. This is shown by comparisons between the results obtained using the proposed method and experimental data obtained on smooth surfaces with and without pressure gradients and heat transfer.

4. While this method for predicting the boundary-layer development in the transition region may be regarded as approximate at the present time because of the paucity of adequate experimental data, it does at least provide a basis for calculations and an insight as to the experimental data that are required for modification and refinement.

METHOD

Boundary-Layer Momentum Equation

5. Basic to the proposed method for calculating the boundary layer behavior in the transition region consists of a step-by-step solution of the boundary-layer momentum equation (reference i):

$$\frac{d\theta}{ds} = \frac{c_f}{2} - \theta\left[\left(\frac{\delta^*}{\theta} + 2\right)\frac{du_e}{u_e\,ds} + \frac{1}{\rho_e}\frac{d\rho_e}{ds} + \frac{1}{R}\frac{dR}{ds}\right] \quad (1)$$

in the transition region.

6. Over a given surface the needed values of the stream properties u_e and ρ_e just outside the boundary layer are obtained from either experimental pressure distribution data or from a calculation scheme which is given in Appendix A.

7. As is usually done, the initial laminar flow is calculated using an appropriate analytical method (Appendix A) up to the point where it is assumed that transition starts. At this point on the surface, the values of the boundary-layer properties such as the skin-friction coefficient (c_f), boundary-layer shape parameter $(\delta^*/\theta)_c$, and the momentum thickness (θ_c) are known. This is sufficient information to start the transition region calculations. The following sections discuss the procedures to be used for calculating the needed skin-friction coefficients and the needed values of δ^*/θ in the transition region.

Skin-Friction Coefficients

8. It [illegible] ance (j) from a large collection of [illegible] incompressible flow that the skin-friction [illegible] transition region varies with Reynolds number according to a law of the form:

$$c_{f_{tr}} = c_{f_{Turb}} - \frac{\text{constant}}{Re_\theta^2} \qquad (2)$$

In the absence of experimental data to confirm or reject this form of the transition region skin-friction law for compressible flows, it will be assumed that the form of Equation (2) is applicable for all cases which are considered herein. It is interesting to point out here, that when Re_θ becomes very large

$$c_{f_{tr}} \approx c_{f_{Turb}} \qquad (3)$$

and the results obtained will therefore fair smoothly into the turbulent zone of a given body shape.

9. The value of the constant in Equation (2) is principally a function of the assumed value of Re_θ at the start of transition, however, it does depend somewhat on the circumstances of the particular calculation. This constant is determined in the following manner. At the assumed point where transition starts

$$c_{f_{Lam}} = c_{f_{tr}} \qquad (4)$$

For the calculated laminar value of Re_θ, a value of $c_{f_{Turb}}$ is determined using either the equations and procedure described in reference (k) or another theory which adequately predicts turbulent boundary-layer skin-friction coefficients. This information is sufficient to determine the value of the constant for a given calculation. It should be pointed out here that since the values of $c_{f_{Lam}}$ and $c_{f_{Turb}}$ are somewhat dependent on heat transfer and pressure gradient, the value of the constant will depend on these quantities. The influence of these effects is, in general, fairly small, and as mentioned before the value of the constant depends mainly on the value of Re_θ at the start of transition. An illustration of several typical transition region skin-friction curves is given in Figure 1, which shows the variation of c_f with Re_θ for incompressible flat plate flow. For this particular case, Figure 2 shows the variation of the constant in Equation (2) with assumed value

of Re_θ at the start of transition.

Boundary-Layer Shape Parameter

10. It can be seen from Equation (1) that in addition to values of $c_{f_{tr}}$, it is necessary to have a means for determining the values of the boundary-layer shape parameter in the transition region. It was shown in reference (h) that transition region boundary-layer velocity profiles from a single parameter family of curves when correlated with the incompressible definition of δ^*/θ (H_{inc}).

11. Using these experimental data, the behavior of $(\delta^*/\theta)_{inc}$ through the transition region was plotted as a function of ΔRe_θ where

$$\Delta Re_\theta = (Re_\theta)_s - (Re_\theta)_{start\ of\ transition} \quad (5)$$

The data are plotted in Figure 3 on a logarithmic scale and a faired curve is shown in Figure 4 on a Cartesian coordinate scale. In view of the inaccuracies inherent in the determination of $(\delta^*/\theta)_{inc}$, the correlation shown in Figure 3 is remarkable. These results indicate that over a wide range of flow conditions, the transition region covers a length of body surface corresponding to an increase in Re_θ of about 1000. The fairly large scatter in the values of $(\delta^*/\theta)_{inc}$ at the end of transition is due to the fact that $(\delta^*/\theta)_{inc}$ for turbulent flow is a function of Re_θ itself, and since these data represent a wide variety of values of Re_θ at the start of transition it is to be expected that $(\delta^*/\theta)_{inc}$ at the end of transition will vary somewhat. It should be pointed out that the calculation scheme given herein accounts for the Reynolds number influence on $(\delta^*/\theta)_{inc}$ at the start of turbulent flow. This is because the method for determining turbulent boundary skin-friction coefficients given in reference (k) takes into account the variation of $(\delta^*/\theta)_{inc}$ on the values of $c_{f_{Turb}}$.

Calculation Procedure

12. The procedure for calculating the boundary-layer development in the transition region for incompressible isothermal flow is straightforward. At an assumed transition point, the values of θ, $c_{f_{Lam}}$, and $(\delta^*/\theta)_{inc}$ are available from the laminar boundary-layer calculations. This information together with the velocity distribution and known geometry is inserted into

Equation (1) and a value of θ may be calculated at some small arbitrary increment of distance s. From the known conditions outside the boundary layer, the value of Re_θ at this new position can then be calculated and the value of ΔRe_θ determined. This value of ΔRe_θ is used with either Figure 3 or 4 to determine the value of $(\delta^*/\theta)_{inc}$. Knowledge of Re_θ at this new point also yields cf_{tr} from Equation (2). The procedure is then repeated in a stepwise manner along the body surface until the end of the body is reached. As mentioned before, the transition region results obtained fair smoothly into the turbulent zone and therefore, this procedure is applicable for the entire body surface downstream of the laminar flow region.

13. For compressible flows with and without heat transfer the procedure must be modified somewhat because Equation (1) requires the use of $(\delta^*/\theta)_c$ rather than $(\delta^*/\theta)_{inc}$. To determine values of $(\delta^*/\theta)_c$ the velocity profile correlation curve given in reference (h) is used in conjunction with Figure 3 or 4. For convenience the velocity profile correlation curve is given herein as faired curves for clarity purposes (Figure 5). The reader is referred to Figure 13 of reference (h) which shows the experimental data from which this set of faired curves was prepared.

14. Values of $(\delta^*/\theta)_c$ for use in Equation (1) are obtained in the following manner. Using the curves shown in either Figure 3 or 4 the value of $(\delta^*/\theta)_{inc}$ is determined at each successive point. This value of $(\delta^*/\theta)_{inc}$ is used with Figure 5 to determine the variation of u/u_e with y/θ_{inc}. Since the value of $(\delta^*/\theta)_c$ is defined as

$$\left(\frac{\delta^*}{\theta}\right)_c = \frac{\int_0^{y/\theta_{inc}} \left(1 - \frac{T_e u}{T\, u_e}\right) d\left(\frac{y}{\theta_{inc}}\right)}{\int_0^{y/\theta_{inc}} \frac{T_e u}{T\, u_e}\left(1 - \frac{u}{u_e}\right) d\left(\frac{y}{\theta_{inc}}\right)} \qquad (6)$$

this integration may only be carried out if the temperature distribution across the boundary layer is known. The following simple expression for the temperature distribution is used (reference k);

$$\frac{T}{T_e} = \frac{T_w}{T_e} - \frac{T_w - T_{ad}}{T_e}\left(\frac{u}{u_e}\right) - \frac{T_{ad} - T_e}{T_e}\left(\frac{u}{u_e}\right)^2 \qquad (7)$$

Values of T_{ad} are obtained from

$$\frac{T_{ad}}{T_e} = 1 + r\,\frac{\gamma - 1}{2}\,M_e^2 \qquad (8)$$

where a mean value of the recovery factor (r) (say r = 0.87), is sufficiently accurate for the present calculations.

15. With the exception of the determination of the values of $(\delta^*/\theta)_c$ for the compressible flow case, the procedure for calculating the boundary-layer behavior in the transition region is the same for both incompressible and compressible flows with and without heat transfer.

16. At this point, it is important to point out the basic assumptions inherent in the procedure described and also how these may affect the validity of the results obtained. Since the system of equations used for calculating the values of $c_{f_{tr}}$ and $c_{f_{Turb}}$ were obtained for the zero pressure gradient case, it is implied that the influence of pressure gradient on c_f is negligible. This is a necessary assumption because experimental information and dependable analytical relations which describe the influence of pressure gradient on the skin friction in the transition region are not yet available. Another consideration is the use of the empirical correlations of the experimental data of reference (h), Figure 5. Although these data represent both incompressible and compressible flows with and without pressure gradients, none of the data examined were obtained under heat-transfer conditions. Despite this fact, it is felt that these correlations can be used for heat-transfer cases because the velocity profile is little affected by heat transfer either to or from the surface (reference k). The influence of heat transfer is taken into account, however, in the determination of $(\delta^*/\theta)_c$ through the temperature profile across the boundary layer.

RESULTS AND DISCUSSION

Zero Pressure Gradient Results

17. The analysis described has been applied to the incompressible flat plate data of reference (1) and also to the

compressible flow data of reference (m). The results of these calculations are shown in Figures 6 to 9. Figures 6 and 8 show comparisons between the predicted and experimental values of $(\delta^*/\theta)_{inc}$ for each of these cases. Calculations of the laminar boundary layer region of these surfaces were not carried out. As would be expected the agreement between the predicted and experimental values of Re_θ and $(\delta^*/\theta)_{inc}$ are good for both cases. Although this is more or less an anticipated result since the empirical correlations were obtained by using these experimental data, it should be pointed out that the validity of the assumed skin-friction law in the transition region is verified because this was not obtained from these data.

Pressure Gradient Results

18. Since it is anticipated that the method for calculating the boundary-layer behavior in the transition region presented herein will have its greatest usage for bodies of revolution with favorable pressure gradient and heat transfer, these illustrations given in this section will deal principally with this combination of circumstances. It should be realized that this is the general case, however, and deviations from this set of conditions such as two-dimensional flow or flows without heat transfer are special cases, and the procedure describe is sufficiently general to encompass many conceivable condition Where modifications to the procedure are needed to cover any special set of conditions as mentioned above, these will be mentioned and the necessary changes indicated.

19. In the absence of detailed experimental data which can be used for comparison purposes, illustrations can only be given for several examples which do not represent true verifications of the procedure.

20. As pointed out in reference (f), transition observations in the NOL Pressurized Range are made by inspecting shadowgraph photographs. The transition "point" is identified by the first appearance of turbulence near the body surface. As pointed out in reference (f) this point is assumed to be the end of transition or the start of fully turbulent flow. Since the point on the body where transition starts is presently of great importance, a modification of the procedure outlined herein has been used to calculate the point on the body surface where transition starts. This procedure consists of assuming a point on a given body upstream of the observed turbulence, and initiating the transition region calculations at this point. The calculations are carried out until the value of $\Delta Re_\theta \approx 1000$. If this point on the body at which this occurs corresponds to the observed turbulence point, the

assumed position where the transition region calculations are started is correct. If not, the calculations are then repeated until agreement between the calculated end of transition and that observed in the photographs is reached. This procedure is illustrated in Figure 10. In this figure the variation of Re_θ with distance along the surface is shown for one of the Pressurized Range "shots" reported in reference (f). Figures 11 and 12 show the results obtained fro two additional firings made in the NOL Pressurized Range.

Transition Results

21. As pointed out previously the results reported in reference (f) are for the end of transition. It is of interest to examine the correlation of transition data presented in this reference on the basis of values of Re_θ at the start of transition. This is shown in Figure 13, where the variation of Re_θ at the start of transition is plotted as a function of the incompressible pressure gradient parameter $\theta^2/\nu_e \, du_e/ds$. It is apparent that the trends indicated by the values of Re_θ at the end of transition are different than those for the start of transition and the values of Re_θ at the start of transition are a good deal lower than those reported for the end of transition.

CONCLUDING REMARKS

22. A method for calculating the development of the boundary layer in the region of transition from laminar to turbulent flow has been presented. This method is based on empirical correlation of a large amount of velocity profile data in the transition region for incompressible and compressible flows with and without pressure gradients. The velocity profile correlations are used in conjunction with the boundary-layer momentum equation to predict the development of the boundary-layer parameters. A number of examples are presented which illustrate the results obtained using the present method and also test its validity for the cases for which experimental data are available. In addition, a method is suggested for calculating the position of the start of transition on a given body surface when the end of transition is experimentally identified by photographic techniques. Several calculations illustrating this procedure are presented.

23. The proposed method can only be regarded as approximate at the present time because of the paucity of detailed experimental data for verification purposes. It does, however, provide a basis for calculations and an insight as to the experimental data which are required for modifications and refinements.

REFERENCES

(a) Lees, L., "The Stability of the Laminar Boundary Layer in a Compressible Fluid," NACA Report 876, 1947

(b) Van Driest, E. R., "Calculation of the Stability of the Laminar Boundary Layer in a Compressible Fluid on a Flat Plate with Heat Transfer," Jour. Aero. Sci., Vol., 10, No. 12, Dec. 1952. pp. 801-813

(c) Dunn, D. W., and Lin, C. C., "On the Stability of the Laminar Boundary Layer in a Compressible Fluid," Jour. Aero. Sci., Vol. 22, No. 7, July 1955, pp. 455-477

(d) Czarnecki, K. R., and Sinclair, A. H., "Preliminary Investigation of the Effects of Heat Transfer on Boundary-Layer Transition on a Parabolic Body of Revolution (NACA RM-10) at a Mach Number of 1.61," NACA TN 3165, April 1954 (see also NACA TN 3166 and 3230)

(e) Higgins, R. W., and Pappas, C. C., "An Experimental Investigation of the Effect of Surface Heating on Boundary-Layer Transition on a Flat Plate in Supersonic Flow," NACA TN 2351, 1951

(f) Witt, W. R., and Persh, Jerome, "A Correlation of Free-Flight Transition Measurements on Various Blunt Nose Shapes by Use of the Momentum-Thickness Reynolds Number," NAVORD Report 4400

(g) Probstein, Ronald F., and Lin, C. C., "A Study of the Transition to Turbulence of the Laminar Boundary Layer at Supersonic Speeds," IAS Preprint No. 596, 1956

(h) Persh, Jerome, "A Study of Boundary-Layer Transition From Laminar to Turbulent Flow," NAVORD Report 4339

(i) Modern Developments in Fluid Dynamics-High Speed Flow, Edited by L. Howarth. The Claredon Press, Oxford

(j) Schlichting, Dr. Hermann, "Boundary-Layer Theory," New York, McGraw Hill Book Co., 1955

(k) Persh, Jerome, "A Theoretical Investigation of Turbulent Boundary-Layer Flow with Heat Transfer at Supersonic and Hypersonic Speeds," NAVORD 3854, 1954

(l) Von der HeggeZijnen, B. G., "Measurements of the Velocity Distribution in the Boundary Layer along a Plane Surface," Rept. 6, Aero. Lab., Tech., H. S., Delft, 1924

(m) Brinich, P. F., and Diaconis, N. S., "Boundary-Layer Development and Skin Friction at Mach Number 3.05," NACA TN 2742, 1952

(n) Lees, Lester and Kubota, Toshi, "Inviscid Hypersonic Flow Over Blunt-Nosed Slender Bodies," Jour. Aero. Sci., Vol. 24, No. 3, March 1957

(o) Cohen, C. B., and Reshotko, Eli, "The Compressible Laminar Boundary Layer with Heat Transfer and Arbitrary Pressure Gradient," NACA TN 3326, 1955

APPENDIX A

Calculation of Pressure Distribution and Laminar Boundary-Layer Region

1. For the examples presented herein, the pressure distribution about a given body shape was obtained from either experimental data or calculated data using the modified Newtonian flow concept (reference n). This concept neglects the presence of the shock wave in front of a given blunt body, and the pressure on the surface is calculated from

$$\frac{c_p}{c_{p\,max}} = \frac{p_o - p_\infty}{p_o' - p_\infty} = \cos^2 \qquad \text{(A1)}$$

up to a point along the contour where the slope of the pressure versus distance along the surface curve is the same as that obtained from a two-dimensional Prandtl-Meyer expansion about the surface.

$$\left.\frac{dp_e}{ds}\right|_{\text{Newtonian}} = \left.\frac{dp_e}{ds}\right|_{\text{Prandtl-Meyer}} \qquad \text{(A2)}$$

2. This point along the surface may be predetermined by solving the following equation;

$$\sin 2\alpha = \frac{\frac{2\gamma}{\gamma-1}\left\{\left[\left(1-\frac{p_\infty}{p_o'}\right)\cos^2\alpha + \frac{p_\infty}{p_o'}\right]^{-\frac{\gamma-1}{\gamma}} - 1\right\}\left[\left(1-\frac{p_\infty}{p_o'}\right)\cos^2\alpha + \frac{p_\infty}{p_o'}\right]}{\left(1-\frac{p_\infty}{p_o'}\right)\left[\frac{2}{\gamma-1}\left\{\left[\left(1-\frac{p_\infty}{p_o'}\right)\cos^2\alpha + \frac{p_\infty}{p_o'}\right]^{-\gamma-1/\gamma} - 1\right\} - 1\right]^{\frac{1}{2}}} \qquad \text{(A3)}$$

From the point along the surface where Equation (A3) is satisfied on downstream to the end of the body, the pressures are determined using the aforementioned Prandtl-Meyer flow relations. Knowing the pressure distribution around the body, the local flow conditions at any point can be calculated using an isentropic expansion from the stagnation point.

3. For the laminar flow region on the examples presented herein, the compressible laminar boundary-layer analysis for axisymmetric flow given in reference (o), was used. The relevant equation for calculating Re_θ (and hence θ) is:

$$\frac{n}{p' \frac{T_o'}{T_e}} = A \left[\frac{T_e}{T_o'}\right]^{-K} \frac{M_e^{1-B}}{R^2} \int_o^{s/L} \left[\frac{T_e}{T_o'}\right]^{K} \frac{R^2}{M_e^{1-B}} \, d\frac{s}{L} \qquad (A4)$$

which has been rearranged for the present analysis to the following form:

$$Re_\theta^2 = A \frac{u_e}{\nu_e} \frac{\lambda}{I} \int_o^s I \, ds \qquad (A5)$$

where

$$I = \left[\frac{T_e}{T_o'}\right]^{K} M_e^{B-1} R^2 \qquad (A6)$$

and A = constant = 0.44

$$K = \frac{\gamma - 1}{2(\gamma - 1)}$$

The value of B is dependent on the wall temperature and is determined from Figure 4 of reference (o). Since all of the flow properties outside the boundary layer are known from previous calculations, the determination of the value of Re_θ at the start of transition means that the value of θ at this point can be deduced. To determine the value of c_f at this point, the following procedure is required. The value of n is determined using

$$n = -\left[\frac{p_o'}{p_e}\right] \frac{1}{R M_e^2} \left[\frac{T_o'}{T_e}\right] \sin 2\alpha \, F \qquad (A7)$$

where

$$F = 0.44 \frac{1}{I} \int_0^s I \, ds$$

and the value of s_w calculated from

$$s_w = \frac{T_w}{T_o'} - 1$$

4. When both n and s_w are calculated Figures 1 and 2 reference (c), may be used to obtain quantities f and

$$\left[\frac{c_{f_w} Re_w}{Nu_w}\right]_{Pr=1}$$

Since

$$c_{f_w} \sqrt{Re_w} = 2f \sqrt{\frac{n}{y}}$$

the value of c_{f_w} and thereby c_{f_e} can be calculated by u

$$c_{f_e} = c_{f_w} \left[\frac{T_e}{T_w}\right]$$

If the heat transfer is desired, this can be obtained i following manner; calculate the value of Nu_w using

$$\frac{c_{f_w} \sqrt{Re_w}}{\left[\frac{c_{f_w} Re_w}{Nu_w}\right]_{Pr=1}} = \frac{Nu_w}{\sqrt{Re_w}}$$

which in turn yields the heat-transfer coefficient, h, thereby q can be calculated from

$$q = k_w \left.\frac{\partial T}{\partial y}\right|_w = h \left[T_{ad} - T_w\right]$$

$$F = 0.44 \frac{1}{I} \int_0^s I \, ds \qquad (A8)$$

and the value of s_w calculated from

$$s_w = \frac{T_w}{T_0'} - 1$$

4. When both s and s_w are calculated Figures 1 and 2 of reference (c), may be used to obtain quantities f and

$$\left[\frac{c_{f_w} Re_w}{Nu_w}\right]_{Pr=1}$$

Since

$$c_{f_w} \sqrt{Re_w} = 2f \sqrt{\frac{s}{F}} \qquad (A9)$$

the value of c_{f_w} and thereby c_{f_e} can be calculated by using

$$c_{f_e} = c_{f_w} \left[\frac{T_e}{T_w}\right] \qquad (A10)$$

If the heat transfer is desired, this can be obtained in the following manner; calculate the value of Nu_w using

$$\frac{c_{f_w} \sqrt{Re_w}}{\left[\frac{c_{f_w} Re_w}{Nu_w}\right]_{Pr=1}} = \frac{Nu_w}{\sqrt{Re_w}} \qquad (A11)$$

which in turn yields the heat-transfer coefficient, h, and thereby q can be calculated from

$$q = k_w \left.\frac{\partial T}{\partial y}\right|_w = h \left[T_{ad} - T_w\right] \qquad (A12)$$

The last needed quantity $(\delta^*/\theta)_c$ can be obtained

$$\left[\frac{\delta^*}{\theta}\right]_c = H_{inc}\left[\frac{T_o'}{T_e}\right] + \left[\frac{T_o'}{T_e} - 1\right] \qquad \text{(A13)}$$

where H_{inc} is given as Figure 6 of reference (o) as a function of n and s_w.

5. The parameters necessary to start the transition region calculations are therefore obtainable using this procedure for calculating the laminar boundary-layer behavior.

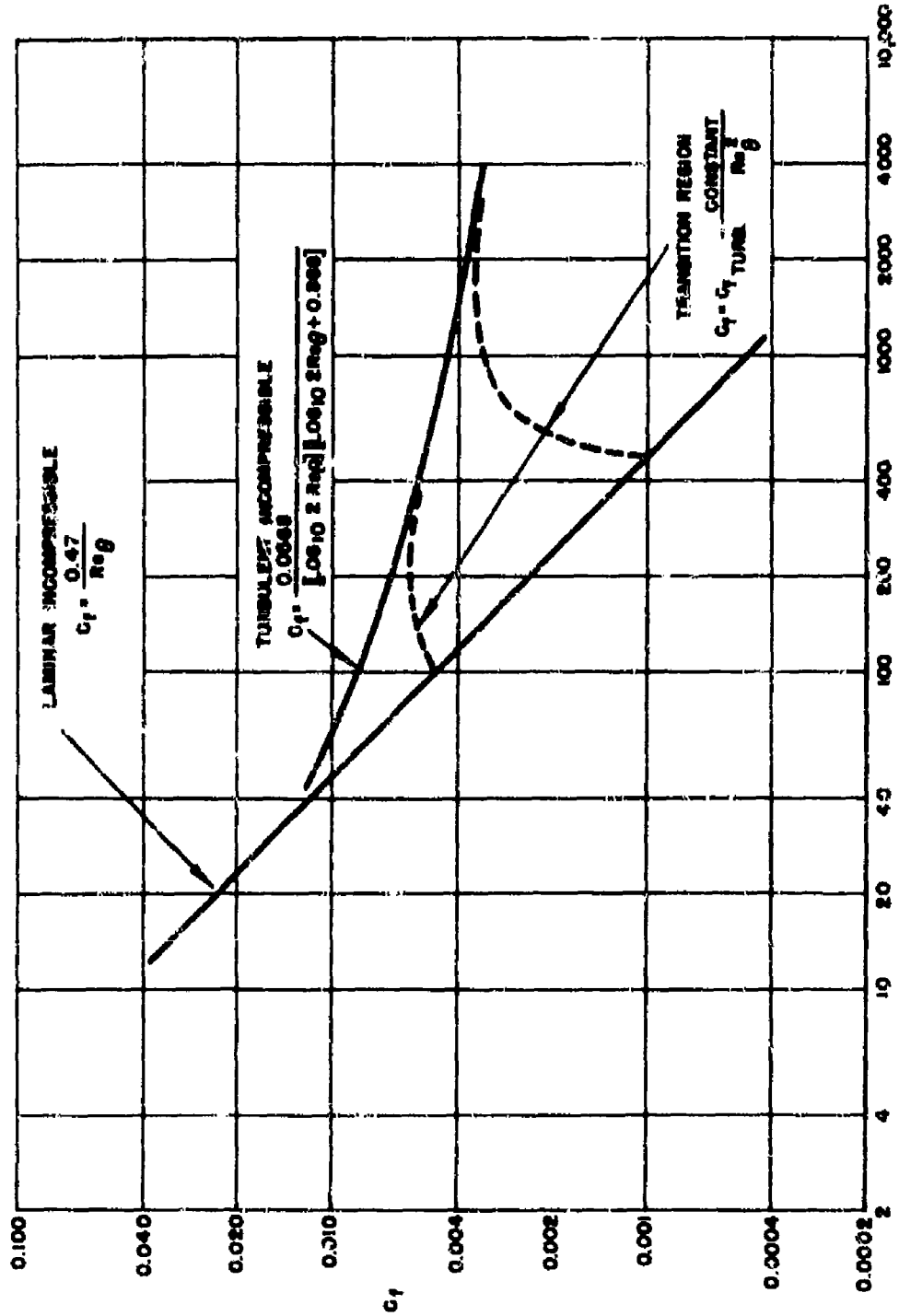

FIG. 1 THE VARIATION OF INCOMPRESSIBLE LOCAL SKIN-FRICTION COEFFICIENTS (c_f) WITH MOMENTUM THICKNESS REYNOLDS NUMBER (Re_θ)

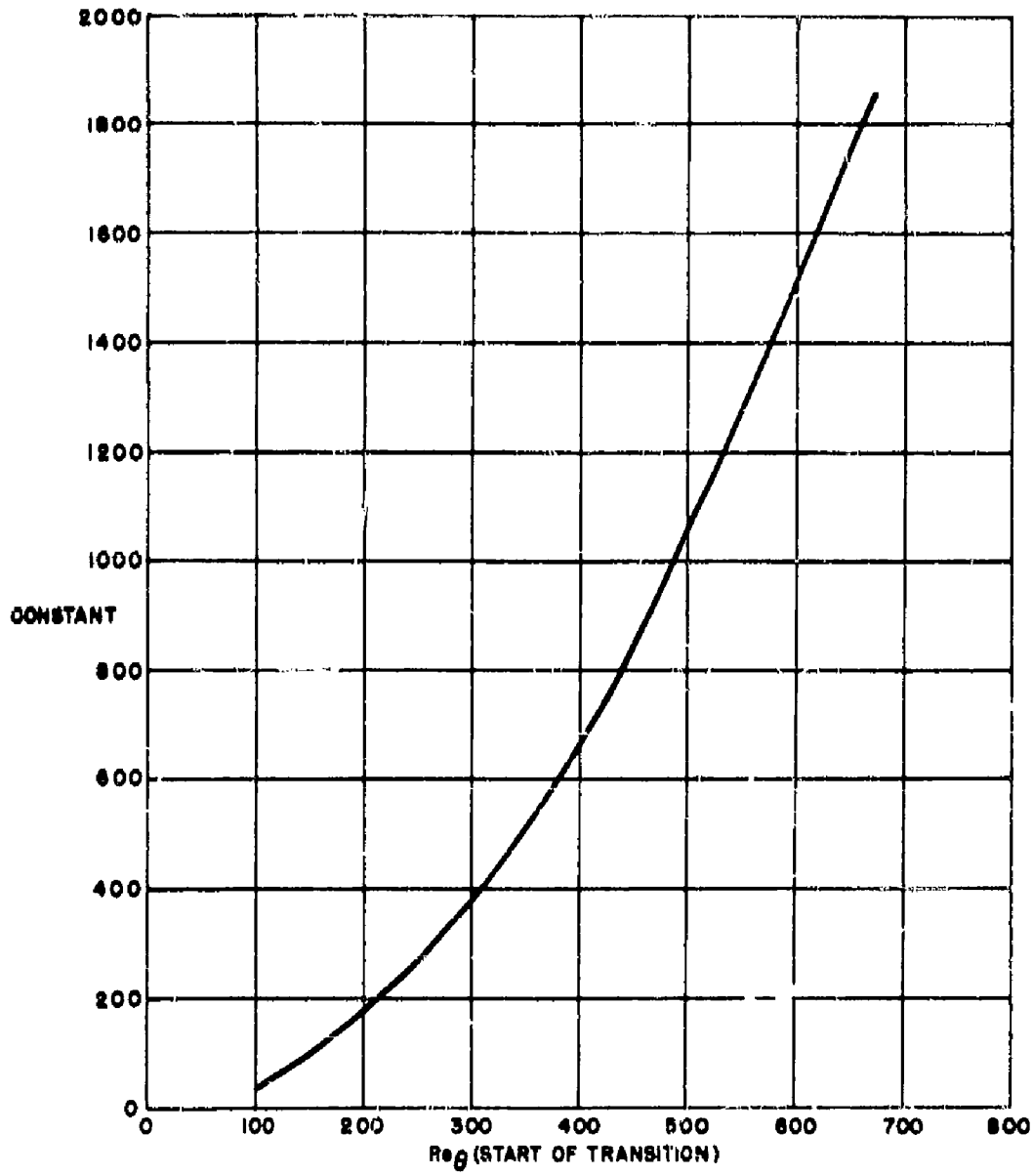

FIG. 2 THE VARIATION WITH Re_θ AT THE START OF TRANSITION OF THE CONSTANT APPEARING IN THE TRANSITION REGION SKIN FRICTION FORMULA FOR INCOMPRESSIBLE FLOW

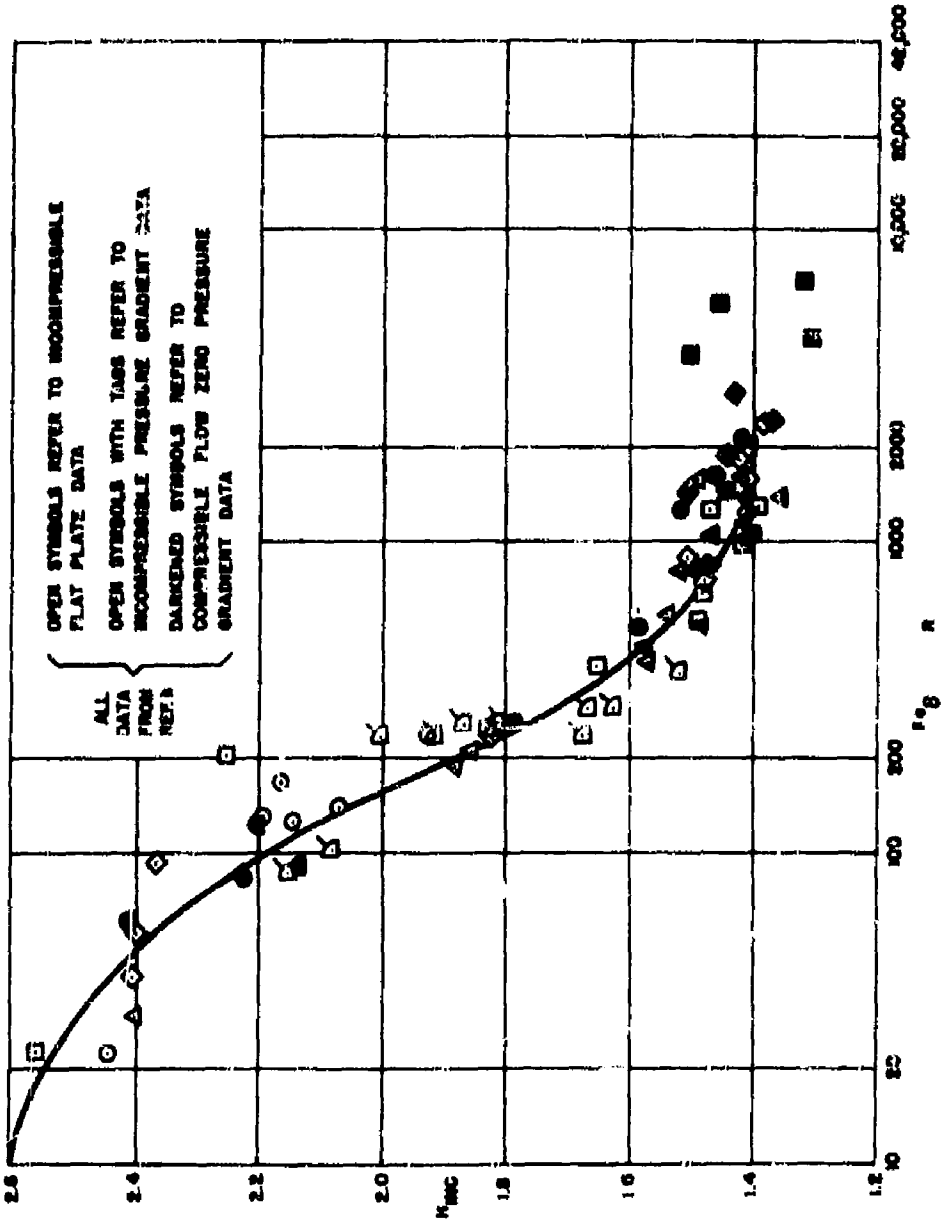

FIG. 3 CORRELATION OF H_{INC} WITH Re_θ IN THE TRANSITION REGION

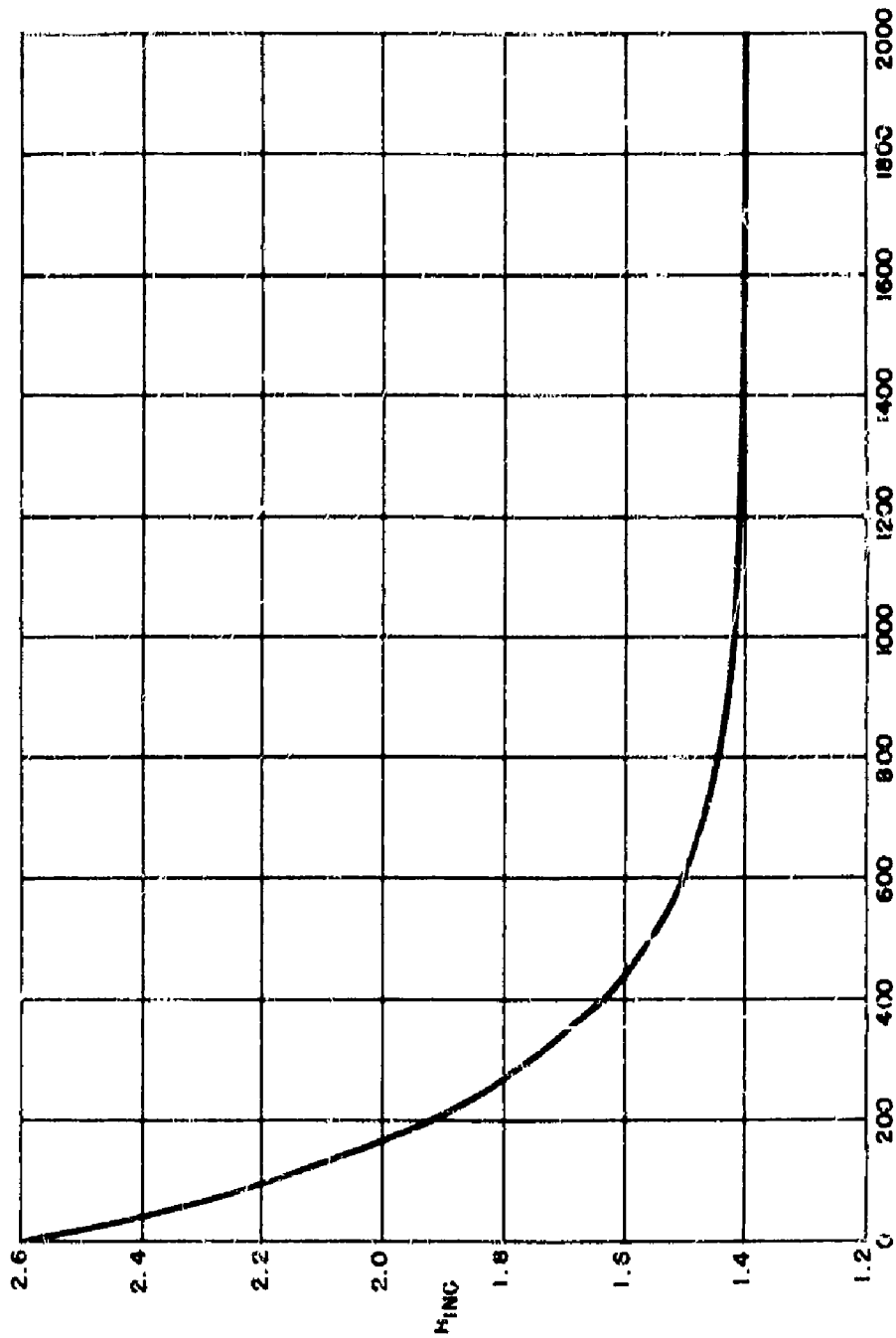

FIG.4 THE VARIATION OF H_{INC} WITH Re_θ IN THE TRANSITION REGION

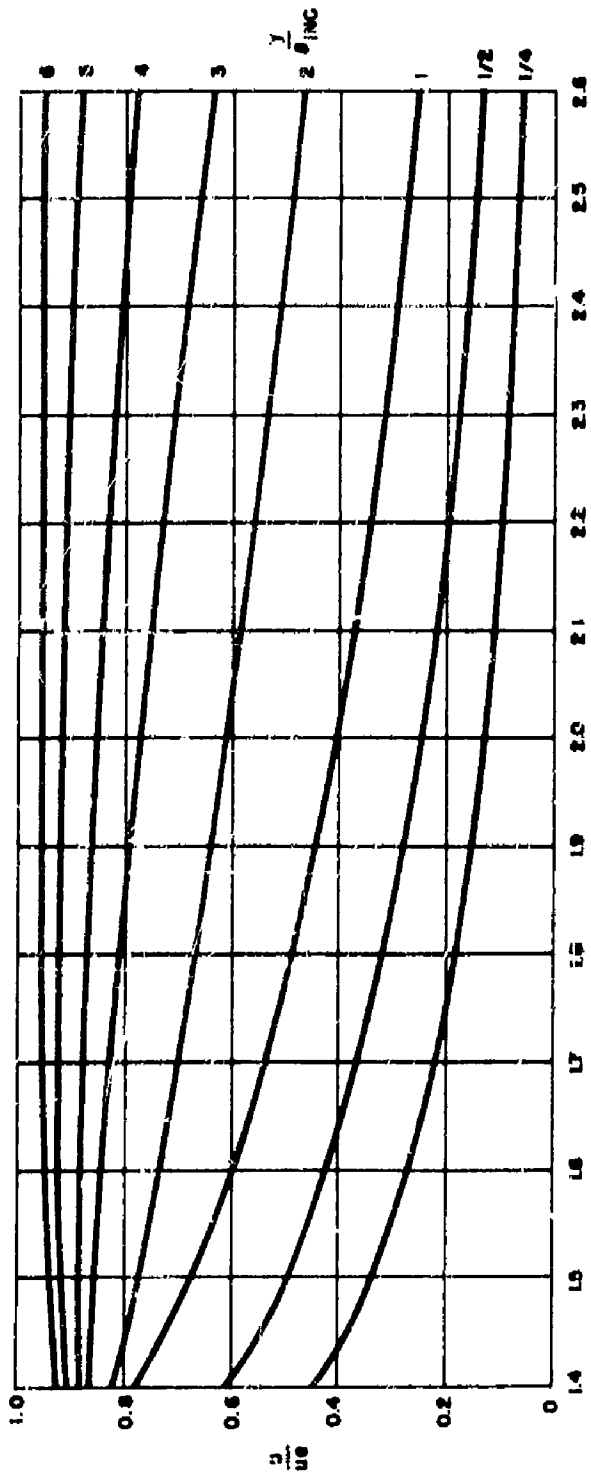

FIG. 5 THE VARIATION OF u/u_e WITH H_{INC} FOR VARIOUS VALUES OF y/θ_{INC} FOR TRANSITION REGION VELOCITY PROFILES

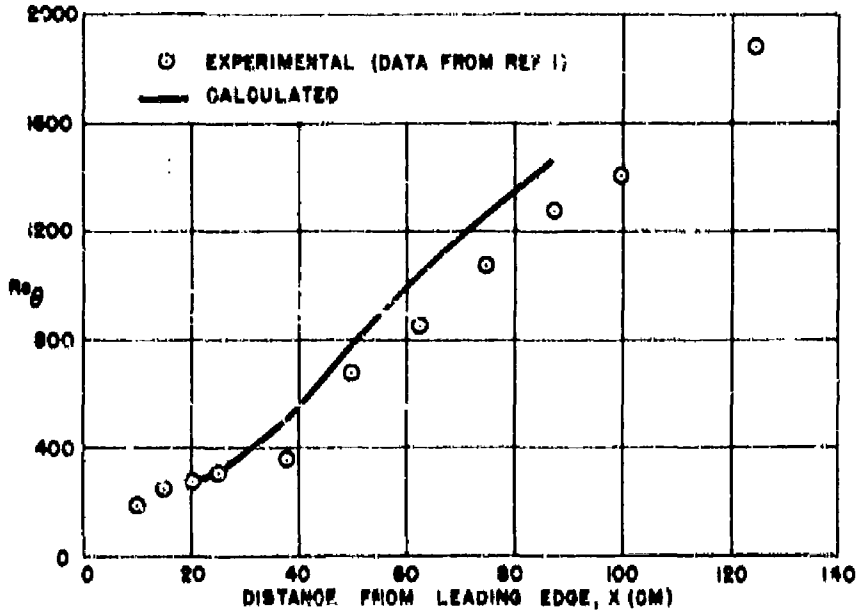

FIG. 6 COMPARISON BETWEEN CALCULATED AND EXPERIMENTAL VALUES OF Re_θ FOR INCOMPRESSIBLE FLAT PLATE FLOW (DATA OF REFERENCE 1)

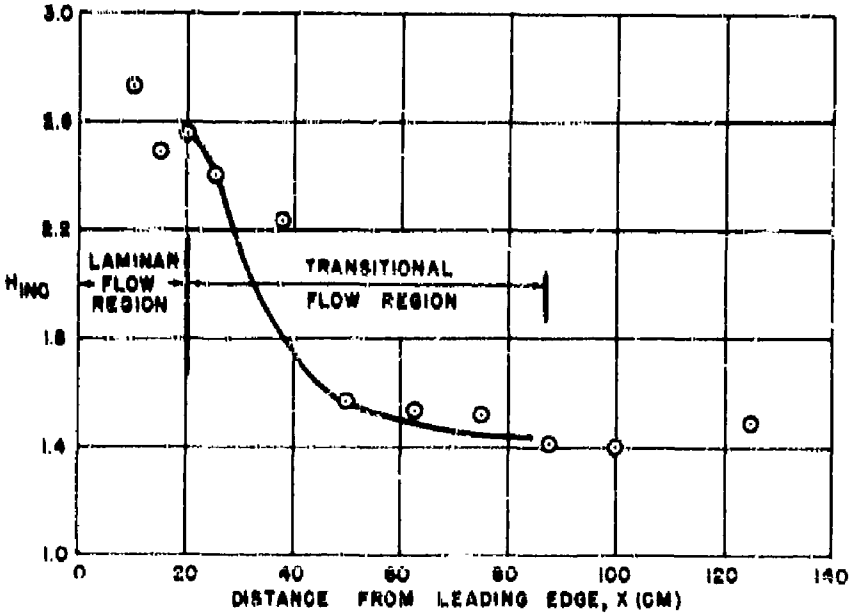

FIG. 7 COMPARISON BETWEEN CALCULATED AND EXPERIMENTAL VALUES OF H_{INC} FOR IMCOMPRESSIBLE FLAT PLATE FLOW (DATA OF REFERENCE 1)

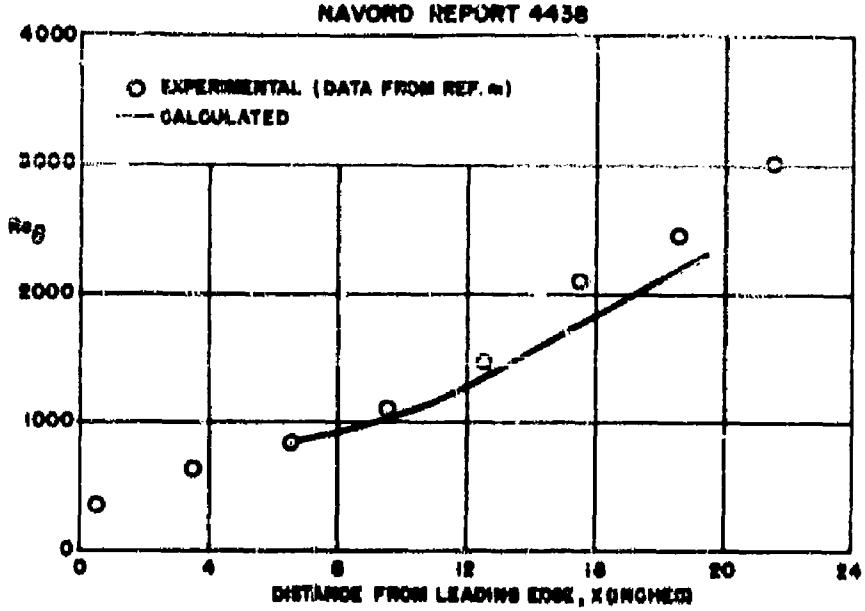

FIG.8 COMPARISON BETWEEN CALCULATED AND EXPERIMENTAL VALUES OF Re_θ FOR COMPRESSIBLE ZERO PRESSURE GRADIENT FLOW (DATA OF REFERENCE m)

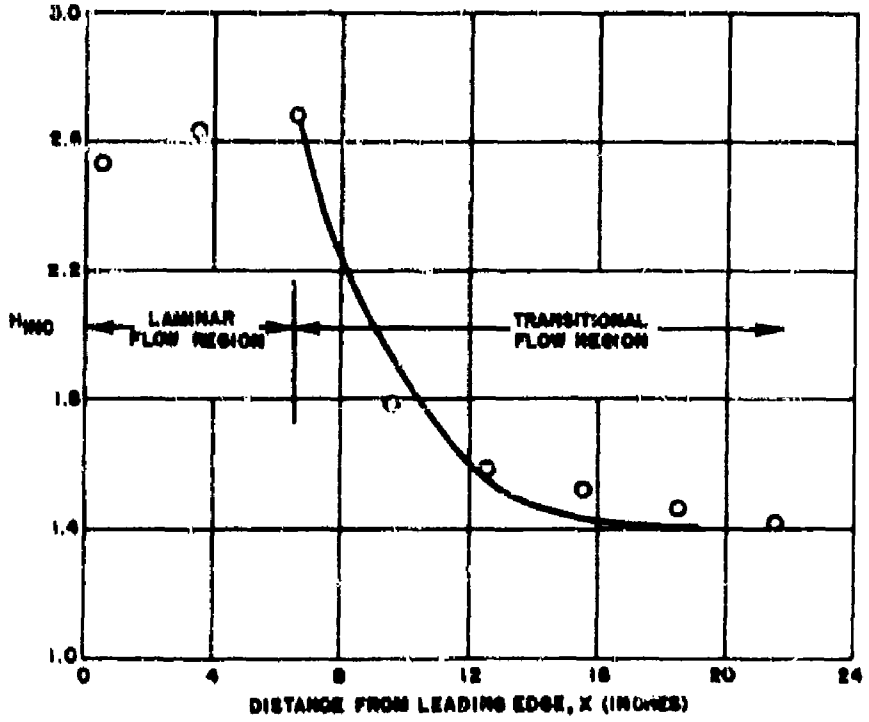

FIG.9 COMPARISON BETWEEN CALCULATED AND EXPERIMENTAL VALUES OF H_{INC} FOR COMPRESSIBLE ZERO PRESSURE GRADIENT FLOW (DATA OF REFERENCE m)

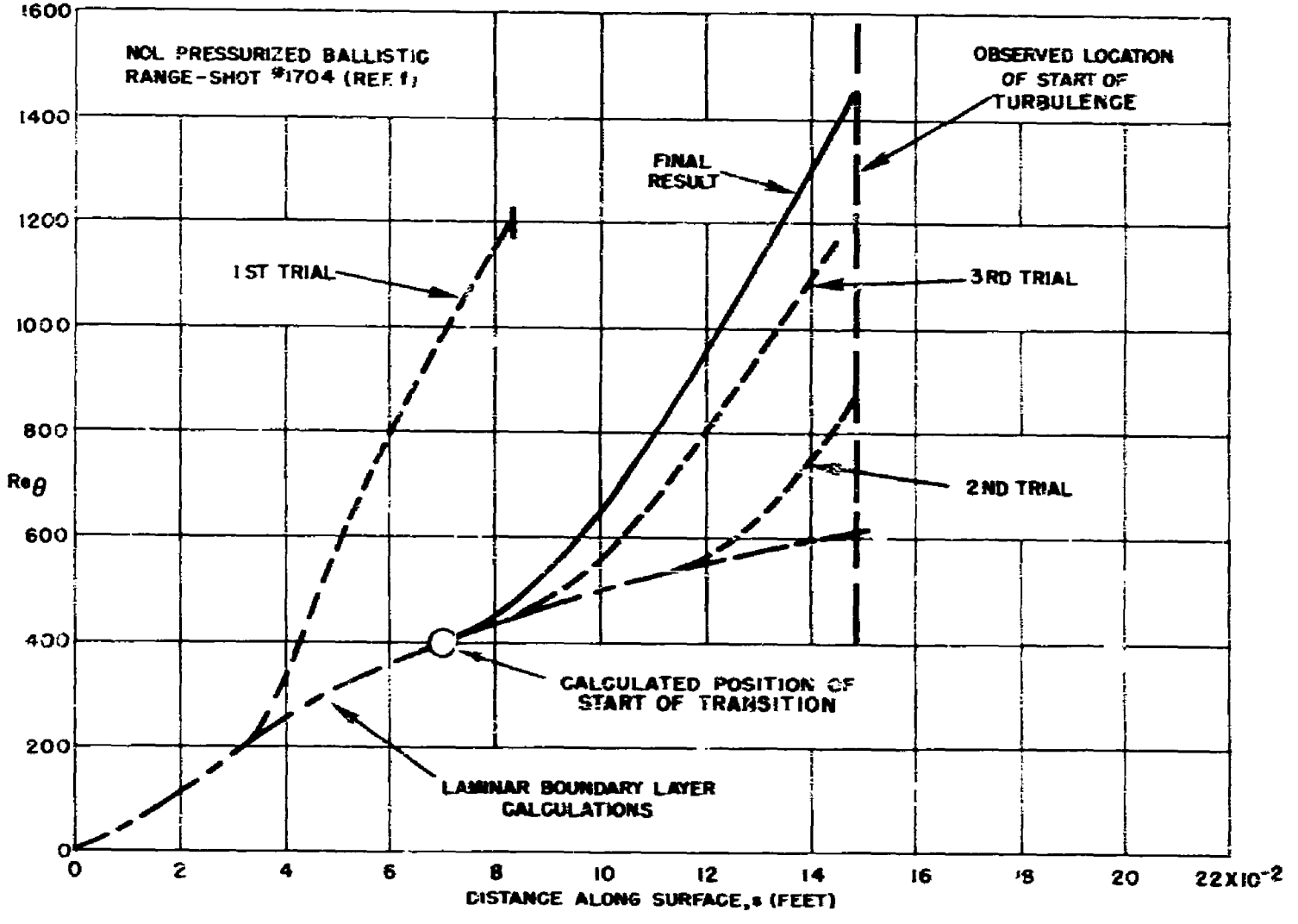

FIG. 10 ILLUSTRATION OF PROCEDURE USED FOR CALCULATING THE START OF TRANSITION FOR NOL PRESSURIZED RANGE DATA

1600

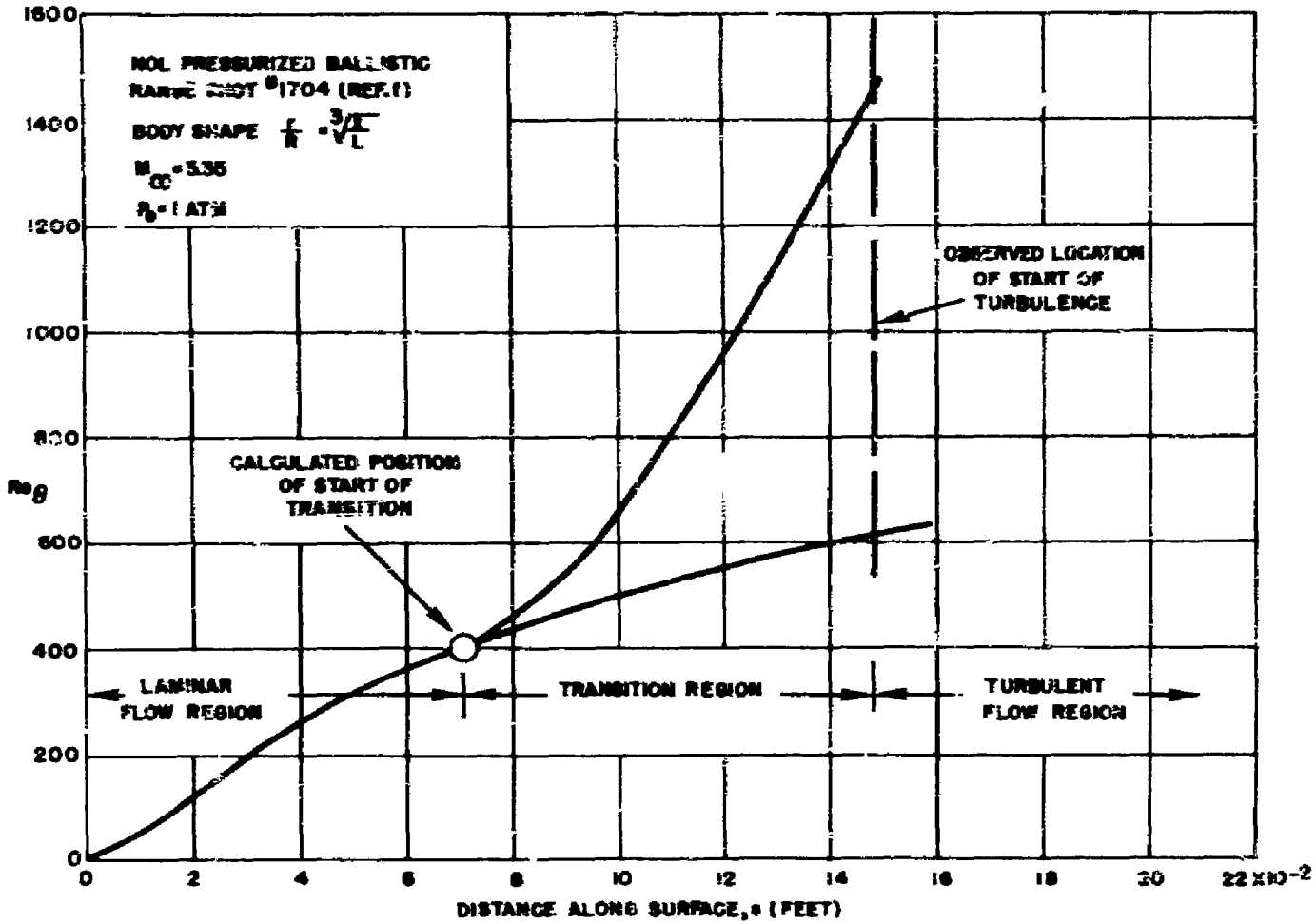

FIG.11 VARIATION OF Re_θ WITH s FOR NOL RRESSURIZED RANGE SHOT #1704 (DATA FROM REFERENCE f)

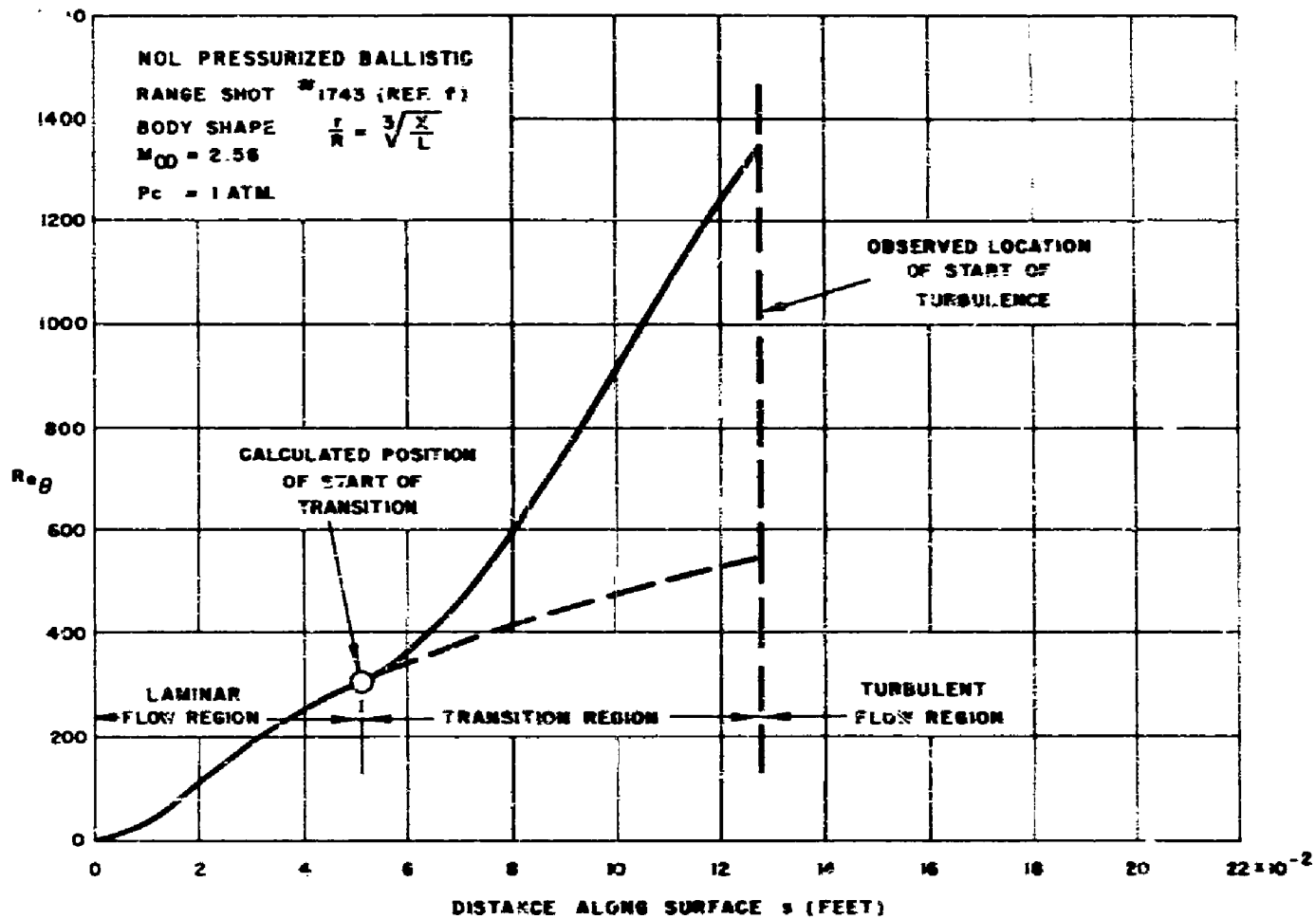

FIG. 12 VARIATION OF Re_θ WITH s FOR NOL PRESSURIZED RANGE SHOT #1743 (DATA FROM REFERENCE f)

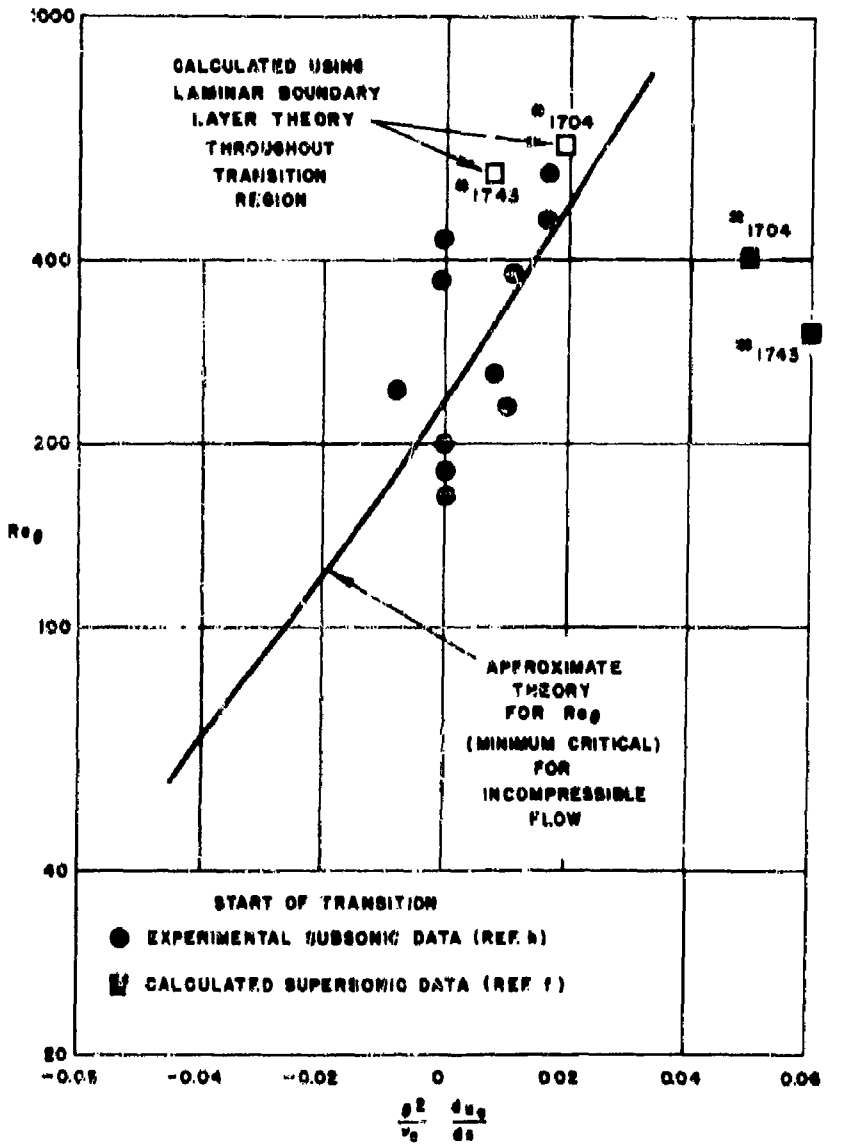

FIG. 13 VARIATION OF CALCULATED VALUES OF R_{e_θ} AT THE START OF TRANSITION WITH $\theta^2/\nu_e \, du_e/ds$ FOR NOL PRESSURIZED RANGE DATA

AEROBALLISTIC RESEARCH DEPARTMENT
EXTERNAL DISTRIBUTION LIST FOR AEROBALLISTIC RESEARCH

No. of Copies	
	Chief, Bureau of Ordnance Department of the Navy Washington 25, D. C.
1	Attn: Ad3
1	Attn: Ree
1	Attn: ReO3
1	Attn: ReSIe
	Chief, BuAer Washington 25, D. C.
3	Attn: TD-414
	Commander, U. S. NOTS Inyokern, China Lake, California
1	Attn: Technical Library
1	Attn: Code 503
	Commander, NAMTC Point Mugu, California
2	Attn: Technical Library
	Superintendent U. S. Naval Postgraduate School Monterey, California
1	Attn: Tech. Reports Section, Library
	Director, NRL Washington 25, D. C.
1	Attn: Code 2021
	Officer in Charge, NPG Dahlgren, Virginia
1	Attn: Technical Library
	Office, Chief of Ordnance Department of the Army Washington 25, D. C.
1	Attn: ORDTU
	Office of the Assistant Secretary of Defense (R and D) Room 3E1065, The Pentagon Washington 25, D. C.
1	Attn: Technical Library

No. of Copies	
	Chief, AFSWP Washington 25, D. C.
1	Attn: Document Library Br.
	Commander, WADC Wright-Patterson AF Base Ohio
5	Attn: WCOSI-3
3	Attn: WCRRD
1	Attn: WCLGH-3
1	Director Air University Library Maxwell AF Base, Alabama
	Commanding General Aberdeen Proving Ground, Md.
1	Attn: Technical Info. Br.
1	Attn: Ballistics Res. Lab.
10	ASTIA Document Service Center Knott Building Dayton 2, Ohio
	NACA High Speed Flight Station Box 273 Edwards AF Base, California
1	Attn: Mr. W. C. Williams
	NACA Ames Aeronautical Laboratory Moffett Field, California
1	Attn: Librarian
	NACA Langley Aeronautical Laboratory Langley Field, Virginia
2	Attn: Librarian
1	Attn: Adolf Busemann
1	Attn: John J. Stack

No. of Copies

NACA
Lewis Flight Propulsion Lab.
21000 Brookpark Road
Cleveland 11, Ohio
1 Attn: Librarian

NACA
1512 H Street N. W.
Washington 25, D. C.
1 Attn: Bortram A. Mulcahy
Chief, Div. of Research Information

Commanding Officer, DOFL
Washington 25, D. C.
1 Attn: Librarian
Room 211, Building 92

Office of Naval Research
Room 2709, T-3 Building
Washington 25, D. C.
1 Attn: Head, Mechanics Br.

Director of Intelligence
Headquarters, USAF
Washington 25, D. C.
1 Attn: AFOIN-3B

Director, DTMB
Aerodynamics Laboratory
Washington 7, D. C.
1 Attn: Library

University of California
Berkeley 4, California
1 Attn: O. J. Maslach, 205-T3
2 Attn: Dr. S. A. Schaaf

Defense Research Laboratory
The University of Texas
P. O. Box 8029
Austin 12, Texas
1 Attn: H. D. Krick, Asst. Dir.

1 Applied Math. & Statistics Lab.
Stanford University
Stanford, California

No. of Copies

University of Michigan
Willow Run Research Center
Willow Run Airport
Ypsilanti, Michigan
1 Attn: Librarian

1 University of Michigan
Ann Arbor, Michigan

APL/JHU
8621 Georgia Avenue
Silver Spring, Maryland
2 Attn: Tech. Rpts. Group

The Ohio State University
Research Foundation
Nineteenth Avenue
Columbus 10, Ohio
1 Attn: Security Officer

CIT
Pasadena 4, California
1 Attn: Aeronautics Department
2 Attn: Jet Propulsion Laboratory
1 Attn: Guggenheim Aeronautical Lab., Aeronautics Library

University of Minnesota
Minneapolis, 14, Minnesota
1 Attn: Mechanical Eng. Dept.

1 BAR
Aerojet-General Corporation
6352 N. Irwindale Avenue
Azusa, California

RAND Corp.
1700 Main Street
Santa Monica, California
1 Attn: Lib., USAF Project RAND

Douglas Aircraft Company Inc.
Santa Monica Division
3000 Ocean Park Boulevard
Santa Monica, California
1 Attn: Chief Engineer

No. of Copies

1 CONVAIR Corp.
A Div. of Gen. Dynamics Corp.
Daingerfield, Texas

1 CONVAIR Corp.
San Diego, California

United Aircraft Corporation
400 Main Street
East Hartford 8, Connecticut
1 Attn: Chief Librarian

Cornell Aeronautical Lab., Inc.
P. O. Box 235, 4455 Genesee St.
Buffalo 21, New York
1 Attn: Librarian

Lewis Flight Propulsion Lab.
21000 Brookpark Road
Cleveland 11, Ohio
1 Attn: Chief, Supersonic Propulsion Division

Armour Research Foundation
10 West 35 Street
Chicago 16, Illinois
2 Attn: Dept. M

Hughes Aircraft Company
Florence Ave. at Teale St.
Culver City, California
1 Attn: Mr. Dana M. Johnson
R and D Technical Library

1 McDonnell Aircraft Corporation
P. O. Box 516
St. Louis 3, Missouri

General Electric Company
Missiles & Ordnance Systems Department
3198 Chestnut Street
Philadelphia, Pennsylvania
2 Attn: Larry Chasen
Manager, Library

No. of Copies

Eastman Kodak Company
Navy Ordnance Division
50 West Main Street
Rochester 14, New York
2 Attn: Mr. W. B. Forman

Lockheed Aircraft Corporation
Missile Systems Division
Van Nuys, California
1 Attn: D. L. N. Wilson

1 Chief, Fluid Mechanics Section
National Bureau of Standards
Washington 25, D. C.

National Bureau of Standards
Washington 25, D. C.
1 Attn: Applied Math. Div.

1 Commanding Officer
Office of Naval Research Br. Off.
Box 39, Navy 100
Fleet Post Office
New York, New York

Langley Aeronautical Laboratory
Langley Field, Virginia
1 Attn: Theoretical Aerodynam. Div.

Case Institute of Technology
Cleveland 6, Ohio
1 Attn: G. Kuerti

Massachusetts Institute of Tech.
Cambridge 39, Mass.
1 Attn: Prof. Joseph Kaye
Room 1-212

The Johns Hopkins University
Charles and 34th Streets
Baltimore 18, Maryland
1 Attn: Dr. Francis H. Clauser

2 Director
Inst. for Fluid Dynamics and Applied Mathematics
University of Maryland
College Park, Maryland

No. of Copies

Commanding Officer and Director
David Taylor Model Basin
Washington 7, D. C.
2 Attn: Hydrodynamics Lab.

Res. and Development Board
Pentagon 3D1041
Washington 25, D. C.
2 Attn: Library Branch

Jet Propulsion Lab.
CIT
4800 Oak Grove Drive
Pasadena 3, California
1 Attn: F. E. Goddard, Jr.
1 Attn: Dr. F. P. Wegener
1 Attn: Mr. J. Laufer
1 Attn: Mr. D. R. Bartz

CIT
Pasadena 4, California
2 Attn: Librarian (Guggenheim Aero. Lab.)
1 Attn: Mr. L. Lees
1 Attn: Prof. M. S. Plesset
1 Attn: Dr. H. W. Liepmann
1 Attn: Mr. A. Roshko
1 Attn: Dr. D. Coles
1 Attn: Mr. Satish Dhawan

University of Illinois
202 E. E. R. L.
Urbana, Illinois
1 Attn: Prof. A. H. Taub

MIT
Cambridge 39, Massachusetts
1 Attn: Project Meteor
1 Attn: Prof. G. Stever
1 Attn: Prof. Dean
1 Attn: Mr. J. Baron
1 Attn: Mr. M. Sweeney, Jr.
1 Attn: Prof. E. Reissner
1 Attn: Guided Missiles Library

Code 2727 (SF)
Room 3134A, Munitions Bldg.
Navy Department
Washington 25, D. C.
1 Attn: Mr. L. Liccini

No. of Copies

New York University
45 Fourth Avenue
New York 3, New York
1 Attn: Prof. R. Courant

Polytechnic Institute of Brooklyn
527 Atlantic Ave.
Freeport, New York
1 Attn: Dr. A. Ferri
1 Attn: Prof. N. J. Hoff
1 Attn: Dr. H. Bloom
1 Attn: Dr. P. Libby

AeroJet-General Corp.
6352 North Irwindale Ave.
Azusa, California
1 Attn: BuAer Representative

Harvard University
Cambridge 38, Massachusetts
1 Attn: Prof. G. Birkhoff
1 Attn: Prof. R. von Mises

Missile Aero. Department
Hughes Aircraft Co.
Culver City, California
1 Attn: Dr. A. M. Puckett

Engineering Res. Inst.
East Engineering Bldg.
Ann Arbor, Michigan
1 Attn: Dir. of Ioing Res.

The Artillery School
Anti-Aircraft & Guided Missiles Branch
Fort Bliss, Texas
1 Attn: Res. & Analysis Sec.

Brown University
Div. of Engr.
Providence, Rhode Island
1 Attn: Prof. R. F. Probstein

Development Section
Chance-Vought Aircraft
Dallas, Texas
1 Attn: Dr. R. H. Wilson